ELSEVIER

Journal of Membrane Science 206 (2002) 165–177

journal of MEMBRANE SCIENCE

www.elsevier.com/locate/memsci

Role of a bulky hydrophobic pendant in a hydrophilic copolymer and the effect of heavy ion irradiation on this copolymer

Shuichi Takahashi [a], Tsutomu Nakagawa [a,*], Masaru Yoshida [b], Masaharu Asano [b]

[a] *Department of Industrial Chemistry, Meiji University, 1-1-1 Higashi-mita, Tama-ku, Kawasaki 214-8571, Japan*
[b] *Department of Material Development, Takasaki Radiation Chemistry Research Establishment, Japan Atomic Energy Research Institute, 1233 Watanuki-machi, Takasaki 370-1292, Japan*

Received 26 February 2001; received in revised form 27 July 2001; accepted 6 August 2001

Abstract

The effect of hydrophilic group composition in methacrylate-based copolymer membranes on water content, the dissolved-oxygen permeation and their handling under hydrated conditions has been investigated. The methacrylate-based copolymer was synthesized by the radical bulk polymerization of monomers having hydrophobic groups, trimethylsilylmethyl methacrylate (TMS) and methyl methacrylate (MMA), with a hydrophilic group, *N*,*N*-dimethyl acrylamide (DMAA). The dissolved-oxygen permeability of these copolymer membranes was correlated to the silicon content and water content in the copolymers. The *d*-spacing of each hydrated membrane increased with the increase of the water content. Furthermore, we attempted heavy ion irradiation of one series of the copolymer membranes. For the heavy ion irradiation, ^{129}Xe ion was used in this investigation. The dissolved-oxygen permeability of the heavy ion-irradiated copolymer membranes became higher compared with that of the untreated membranes. The *d*-spacing and flexibility of membrane scarcely changes by heavy ion irradiation. The dissolved-oxygen permeability coefficient of a part of Xe ion-irradiated membrane exceeded the lowest desired oxygen permeability coefficient line for supplying the oxygen to cornea.

Keywords: Methacrylate-based copolymer; Water content; Dissolved-oxygen permeability; Heavy ion irradiation

1. Introduction

In the polymer medical field, polymeric membranes exhibiting high permeability for oxygen and dissolved-oxygen are required for materials, such as contact lenses (CL) or artificial lungs, which must be swelled with the water to fit the human body [1]. It is commonly known that the wettability of CL has an effect on the wearing comfort of CL [2]. Therefore, research to improve CL should focus on the development of a polymer that has both high gas permeability and high water content. Existing hydrogel or hydrophilic polymers, which are claimed to be useful as CL materials, are derived almost exclusively from hydrophilic monomers, such as 2-hydroxyethyl methacrylate (HEMA) or *N*-vinyl pyrrolidone (NVP) [3–7]. The water content of these materials, in general, ranges from 38 to 75%. Also, their oxygen permeability, which depends exclusively on the water content, falls in the range of 8–40 Barrer. The water content of these materials, in addition, depends on the presence of hydrophilic groups, such as alcohols, carboxylic acids, amides and sulfonic acids [8]. The swollen equilibrated state results from

* Corresponding author. Tel.: +81-44-934-7211; fax: +81-44-934-7906.
E-mail address: nakagawa@isc.meiji.ac.jp (T. Nakagawa).

0376-7388/02/$ – see front matter
PII: S0376-7388(01)00778-5

a balance between the osmotic driving forces that cause the water to enter the hydrophilic polymer and the forces exerted by the polymer chains in resisting expansion. In general, there are two approaches for the preparation of a hydrophilic membrane with high oxygen permeability [8,9]. The first one involves the development of higher water content materials. The high water content CL material increases the supply of oxygen to the cornea. The second one involves the copolymerization of methacrylate containing a bulky pendant or polydimethylsiloxane (PDMS) with hydrophilic monomers [8–11]. PDMS, which possesses a high oxygen permeability that is about 70 times higher than that of the poly(HEMA), has been extensively investigated for use in CL materials [12].

In these swollen membranes, it is well known that the water taken in by a membrane is classified into three states, such as non-freezing water, freezing bound water and free water [13,14]. The water that shows a first-order phase transition, such as crystallization, is called the freezing water. Moreover, the freezing water was classified into two descriptions: free water and freezing bound water. The above-mentioned water types are defined by the transition temperature. At a given cooling rate, the free water crystallized at about 255 K and the freezing bound water at around 230 K. The water that never crystallized even at 130 K was defined as the non-freezing water. However, it is difficult to classify freezing water in the freezing bound water and the free water only by a DSC measurement [13–17]. In this study, therefore, the experimental data were analyzed using the two-state model: non-freezing water and freezing water (freezing bound water + free water). The effect of the water content or the dissolved-oxygen permeability on the composition of the hydrophilic group in the copolymer membranes was investigated in detail. The copolymers used in this study were synthesized by the radical bulk copolymerization of a monomer having a bulky hydrophobic group (trimethylsilyl group) with the hydrophilic monomer, *N*,*N*-dimethyl acrylamide (DMAA) [7,9,10,18,19]. The relationship between the bulky hydrophobic group and water in the copolymer membrane was investigated.

In recent years, heavy ion irradiation has been utilized and studied in many fields, such as nuclear fusion, medical, material technology or other scientific fields [20–23]. Previously, the authors reported the effect of heavy ion irradiation on the gas permeation of a PET membrane [24]. As a result, pores were formed in the PET membrane by heavy ion irradiation of a constant condition. Their gas permeation in the dried state increased and exhibited a Knudsen flow. Recently, the hydrophilic membranes having high oxygen permeability are required in medical fields and other scientific fields. We expected that the dissolved-oxygen permeability would increase by heavy ion irradiation and considered its application for CL and artificial dialysis membrane. Moreover, the effect on the dissolved-oxygen permeability of a membrane following heavy ion irradiation had not been reported as yet. Therefore, we attempted to investigate the effect of heavy ion irradiation on the dissolved-oxygen permeability. For ion irradiation, $^{129}Xe^{23+}$ (Xe ion) was supplied from a cyclotron. The dissolved-oxygen permeability of the heavy ion-irradiated copolymer membranes became higher compared with that of the untreated membranes.

2. Experimental

2.1. Materials

Trimethylsilylmethyl methacrylate (TMS; Chisso Corporation), methyl methacrylate (MMA; Junsei Chemical Co. Ltd.) and DMAA (Kohjin Co. Ltd.) were purified by distillation under vacuum prior to use. Their structures are shown in Fig. 1. α,α′-Azobis(isobutyronitrile) (AIBN) purchased from Junsei Chemical Co. Ltd., was used as the initiator.

2.2. Synthesis of copolymers

All copolymers were synthesized by a radical polymerization technique with AIBN as the initiator. The monomers and initiator were placed in a glass ampule that was connected to a vacuum line, the reactants degassed and then sealed under vacuum. The polymerization proceeded at 55 °C for 12 h. The products were precipitated from a large amount of chloroform. These copolymers were reprecipitated three times from chloroform and *n*-hexane to remove any excess

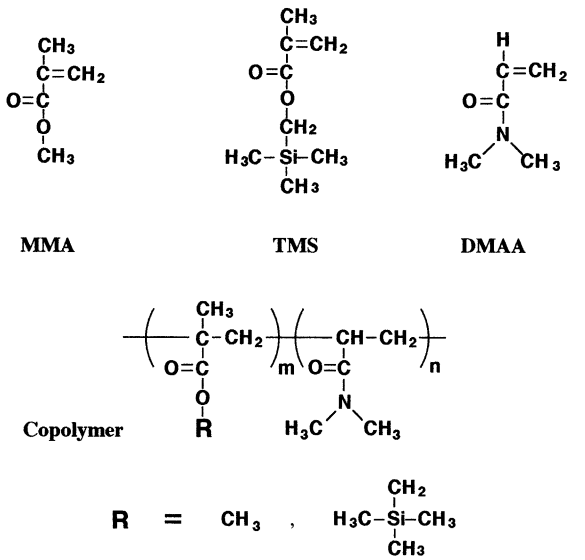

Fig. 1. Structures of MMA, TMS, DMAA and copolymers.

monomer and oligomer and then dried under vacuum for over 24 h. The mole fraction of DMAA in the polymers, that is, DMAA content, was calculated from the nitrogen content that was determined by elemental analysis using the combustion method. These were listed in Table 1.

2.3. Preparation of membranes

Purified copolymers were dissolved in chloroform, then cast on a horizontal glass plate. When the DMAA content in the copolymer was very high, a Teflon plate was used for the casting method. The thickness of dried membranes used in the gas permeation measurement and was approximately 80–100 μm. In the dissolved-oxygen permeation measurement, five membranes with a thickness ranging from 50 to 250 μm (about 50, 100, 150, 200 and 250 μm), for individual synthesized polymers, were prepared in order to negate the effect of the boundary layer [1]. The true permeability coefficient, which considered the boundary layer effect, was calculated by changing the membrane thickness. The details are described in the following paragraph.

For heavy ion irradiation, moreover, copolymer membranes with a thickness of 50 μm were fabricated. This thickness takes into consideration that the heavy ion used in this study was able to cause enough damage to the copolymer network.

Table 1
Characterization of PMMA, PTMS, PDMAA, poly(MMA-co-DMAA) and poly(TMS-co-DMAA) membranes

Sample	DMAA content (mol%)[a]	Water content (wt.%)[b]	T_g (°C)[c]	*d*-Spacing dried state (Å)[d]	*d*-Spacing hydrated state (Å)[d]
PMMA	0.0	1.0	104	5.4	–
90/10-MMA/DMAA	6.4	2.2	104	5.1	–
70/30-MMA/DMAA	20.7	20	113	5.4	5.4
60/40-MMA/DMAA	34.9	42	114	5.4	6.2
50/50-MMA/DMAA	40.3	64	108	5.9	7.4
40/60-MMA/DMAA	51.4	81	108	5.9	9.2
30/70-MMA/DMAA	56.1	Soluble	115	–	–
10/90-MMA/DMAA	73.5	Soluble	113	4.6	–
PDMAA	100	Soluble	117	4.7	–
PTMS	0.0	0.7	77.9	5.3	–
90/10-TMS/DMAA	11.5	0.8	76.2	5.5	–
70/30-TMS/DMAA	29.3	2.9	81.6	5.8	5.4
60/40-TMS/DMAA	37.8	7.3	86.5	5.3	5.4
50/50-TMS/DMAA	47.5	12	87.5	5.6	5.6
40/60-TMS/DMAA	56.8	40	90.0	5.4	6.1
30/70-TMS/DMAA	65.2	65	97.1	5.4	9.8
10/90-TMS/DMAA	80.4	Soluble	102	5.0	–

[a] Determined nitrogen content in the copolymer by elemental analysis using the combustion method.
[b] $(W - W_0)/W$, W: weight of the water-swollen membrane; W_0: weight of the dried membrane.
[c] Determined by DSC at a heating rate of 20 °C/min.
[d] Determined by WAXD using Bragg's equation, $n\lambda = 2d \sin\theta$ (Cu Kα, $\lambda = 1.54$ Å).

2.4. Characterization of membranes

The water content was calculated from the following equation:

$$\text{Water content (\%)} = \frac{W_1 - W_0}{W_1} \times 100 \quad (1)$$

where W_1 is the weight of the water-swollen membrane and W_0 is that of the completely dried membrane. The water-swollen membrane was blotted to remove excess water. The measurement of the weight of that (W_1) was repeated until a constant weight was obtained. The *d*-spacing was measured in the dried and hydrated state by wide angle X-ray diffraction (WAXD; Rigaku RINT-1200) using Bragg's equation, $n\lambda = 2d \sin\theta$ (Cu Kα, $\lambda = 1.54$ Å). The calculation of molecular weight was done using gel permeation chromatography (GPC; Tohsoh HLC-8020). The weight average molecular weight (M_w) and number average molecular weight (M_n) were determined on the basis of a polystyrene calibration. Tetrahydrofuran (THF) was used as carrier solvent. The carrier flow rate was 1 ml/min. A Fourier transform infrared spectrometer (FT-IR; Jasco FT-IR-7300) was used to obtain the IR spectrum of the untreated and the ion-irradiated copolymer membranes.

2.5. Oxygen permeability measurement in the dried and hydrated state

Oxygen permeability in the dried state was determined by vacuum-pressure and time-lag methods. The apparatus for the gas permeability measurement has been schematically described and the procedure described elsewhere [25]. The gas permeability measurements were carried out for pure O_2 at 35 °C. The temperature was controlled to ±0.1 °C. The experimental method used in this study was an adaptation of the vacuum gas transmission technique using a MKS Baratron model 310 BHS-100 SP pressure transducer at <1 atm upstream pressure. The coefficient of variation of the gas permeability examined in this study was <±3%.

The dissolved-oxygen permeability in the hydrated state was measured using an oxygen electrode according to the experimental method developed by Minoura et al. [26]. In this method, a sample membrane is directly attached to the cathode in a 0.5 N KCl solution. To prevent direct contact between the sample and the KCl solution, the sample was tightly inserted between polystyrene film, whose oxygen permeability coefficient is already known. The apparent permeability coefficient of the sample (P_2) is calculated using the following equation:

$$\frac{L_{121}}{P_{121}} = \frac{2L_1}{P_1} + \frac{L_2}{P_2} \quad (2)$$

where L_{121} is the total thickness of the laminated membrane and L_1 and L_2 the thickness of the polystyrene film (40 μm) and copolymer sample, respectively. L_2 was measured by micrometer before the oxygen electrode measurement. P_1 is the oxygen permeability coefficient of polystyrene film (1.2×10^{-10} cm^3 (STP) cm/(cm^2 s cm Hg)). P_{121} value was measured using this oxygen electrode. The apparent dissolved-oxygen permeability calculated using Eq. (2) increased with increased membrane thickness. This was interpreted as being caused by boundary layer resistance, which exists between the sample membrane and the water. Consequently, the true dissolved-oxygen permeability coefficients were calculated using the following equation from five data points of the apparent permeability coefficients which were measured from five membranes, respectively, ranging in thickness from 50 to 250 μm in order to negate the effect of the boundary layer [1,27].

$$\frac{1}{P_g} = \frac{1}{P_{true}} + \left(\frac{1}{R}\right)\left(\frac{1}{d}\right) \quad (3)$$

The above equation yields the true dissolved-oxygen permeability coefficient (P_{true}) at infinite thickness from the apparent one (P_g) of a membrane of diverse thickness (d). The term ($1/R$) is the sum of the resistances of the boundary layers. In heavy ion-irradiated membranes, the measurement of the dissolved-oxygen permeability in the hydrated state was carried out three times using above Eq. (2) because the thickness of the ion-irradiated membrane was only 50 μm. Therefore, the results of this experiment were shown with error bar.

2.6. DSC measurements

The glass transition temperature (T_g) was determined using a Perkin-Elmer DSC-7 at a heating rate of 20 °C/min. The phase transition of water sorbed in the membrane was also evaluated using a Perkin-Elmer

DSC-7. The sample weight was about 5 mg and the phase transition of water sorbed in the membrane was estimated in the temperature range between 153 and 293 K at heating and cooling rates of 5 °C/min. An aluminum sample pan was used, whose surface had previously been treated with boiled water in order to avoid the reaction of the aluminum and water, during heating. The membranes were stored in water at 35 °C for over 24 h. After blotting off the excess water on the membrane, the sample pan was sealed to prevent water vaporization.

2.7. Heavy ion irradiation

For heavy ion irradiation, the synthesized copolymer membranes of 50 μm thickness were cut into 40 mm × 40 mm squares and then attached to 50 mm × 50 mm × 1 mm glass plates. Apparatus for the heavy ion irradiation was illustrated elsewhere [24]. The chamber for the formation of ion-track pores in the membrane, which is connected with the azimuthally varying field (AVF) cyclotron in the Takasaki ion accelerators for advanced radiation applications (TIARA), Japan Atomic Energy Research Institute (JAERI), Japan, is new and was designed for alternate use of turntable-type and roll-type film-carrying systems. Following the heavy ion beam transported from the AVF cyclotron, the geometry and distribution of the heavy ion beam were measured by both a three-wire profile monitor (Irie Co. Ltd., Tokyo, Japan) and a charge coupled device (CCD) camera. The widespread occurrence of heavy ions was controlled by a combination of defocusing with a quadruple electromagnet and collision with metal foils, such as Al, Ta and Cu for scattering. The film-carrying system of a turntable-type can irradiate six square films at the same time.

In this study, $^{129}Xe^{23+}$ (450 MeV) was supplied from the fixed cyclotron. The fluence (the number of irradiated ions per unit area) and the irradiation times were 3×10^{10} ions/cm^2 and 200 s, respectively.

3. Results and discussion

3.1. Characterization

The chemical structures of the synthesized copolymers (poly(MMA-co-DMAA) and poly(TMS-co-DMAA)) are shown in Fig. 1. All of these membranes were colorless and transparent in the dried state. The homopolymer of TMS (PTMS) was hydrophobic and brittle in the dried state. However, the homopolymer of MMA (PMMA), the homopolymer of DMAA (PDMAA) and the copolymer of TMS and DMAA were not brittle in that state. The physical properties of these copolymers and homopolymers are listed in Table 1. The designations of poly(MMA-co-DMAA) and poly(TMS-co-DMAA) in subsequent tables and figures, respectively, are indicated for convenience as MMA/DMAA and TMS/DMAA with proportion of polymerization. The water content of both copolymers increased with an increase in the DMAA content of the copolymer. The increasing water content in poly(MMA-co-DMAA) and poly(TMS-co-DMAA) depends on the number of hydrophilic groups, that is, on that of DMAA content. We believe that the water content of poly(TMS-co-DMAA) gradually increases up to about 50 mol% of DMAA content due to the existence of bulky hydrophobic pendants containing the trimethylsilyl group. The glass transition temperature (T_g) of all copolymers was a single peak, which increased with the increase in the DMAA content. This means that each series of poly(MMA-co-DMAA) and poly(TMS-co-DMAA) do not have a micro-phase separation structure. The most prominent WAXD peak in the spectra of an amorphous glassy polymer is often used to estimate the average interchain spacing distance (*d*-spacing). These values were also calculated using the Bragg's equation and are listed in Table 1. The *d*-spacing of poly(MMA-co-DMAA) and poly(TMS-co-DMAA) in the dried state scarcely changed up to about 50 and 65 mol% DMAA content, respectively. However, the *d*-spacing of the hydrated membranes increased with the increase of water content. It is considered that the existence of water, which is independent of interaction with the hydrophilic group, spread polymer-chain space. The molecular weights of the polymers synthesized in this study are shown in Table 2. All the molecular weight distributions of the polymers exhibited a single peak. The M_n and M_w of the synthesized polymers decreased with an increase in the DMAA content in each copolymer. At the higher molecular weight, such as for $M_n > 10^5$, however, when the concentration of the chain ends is low, the diffusivity is relatively independent of the molecular weight [28,29]. That is

Table 2
Results of GPC measurements for synthesized polymers

Sample	$M_n \times 10^4$	$M_w \times 10^4$	M_w/M_n ratio
PMMA	87	310	3.5
70/30-MMA/DMAA	20	56	2.8
50/50-MMA/DMAA	25	78	3.1
30/70-MMA/DMAA	15	61	4.1
PTMS	130	1500	11.5
90/10-TMS/DMAA	60	1100	19
30/70-TMS/DMAA	54	650	12
50/50-TMS/DMAA	52	510	9.8
30/70-TMS/DMAA	36	260	7.4

to say, we consider that the oxygen permeability does not change by decreasing the molecular weight in this case. The M_w/M_n ratio of poly(MMA-co-DMAA) series changed in the range of 2.5–4. This means that the molecular weight distribution is sharp. That of TMS was 11.5. The molecular weight was very high, but the M_w distribution was broad. Incidentally, it was not possible to measure the molecular weight of PDMAA because the PDMAA did not dissolve sufficiently in the carrier solvent (THF). The monomer reactivity ratio of each copolymer, which was determined by the Fineman–Ross method, was r_1(DMAA) < 1 ($r_1 = 0.67$), r_2(MMA) > 1 ($r_2 = 1.61$) in poly(MMA-co-DMAA) and r_1(DMAA) < 1 ($r_1 = 0.55$), r_2(TMS) < 1 ($r_2 = 0.80$) in poly(TMS-co-DMAA), respectively. We considered that each copolymer in this study is comprised of a random copolymer by radical polymerization. In poly(MMA-co-DMAA), however, the polymerization of MMA is suspected to preferentially occur because the monomer reactivity ratio of MMA to DMAA is 1.61. In poly(TMS-co-DMAA), the structure is comparable to the regular copolymer due to $r_1 r_2 \leq 1$.

3.2. Oxygen permeation properties in the dried state

The above-mentioned analogy related to the copolymer structure is confirmed by the oxygen permeability measurement in the dried state. The relationship between the DMAA volume fraction and oxygen permeability coefficients of the copolymer membranes in the dried state at 35 °C is shown in Fig. 2. The gas permeability coefficients of the homogeneous blend and random copolymers follow a simple mixing rule,

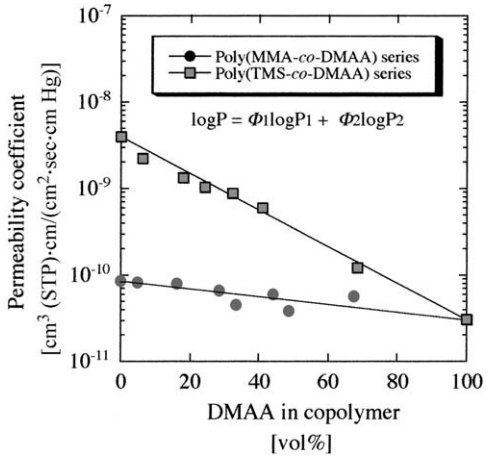

Fig. 2. Relationship between DMAA volume fraction and oxygen permeability coefficients of copolymer membranes in the dried state at 35 °C. Φ_1: The volume fraction of component 1 ($\Phi_2 = 1 - \Phi_1$). P_1, P_2: The permeability coefficients of components 1 and 2.

as shown by the following equation.

$$\log P = \Phi_1 \log P_1 + \Phi_2 \log P_2 \quad (4)$$

where P_1 and P_2 are the permeability coefficients of components 1 and 2 and Φ_1 and Φ_2 the volume fractions of components 1 and 2, respectively. Gas permeability of the PDMAA membrane in the dried state is lower than that of the PTMS and PMMA membranes due to having a strong hydrogen bond in the dried state. As the DMAA content increased, the oxygen permeability of both copolymers gradually decreased and approached the oxygen permeability of the PDMAA because the hydrogen bond part increased with increasing the DMAA content in the copolymer. These results mean that these copolymers are random copolymers because the gas permeability of the poly(MMA-co-DMAA) and poly(TMS-co-DMAA) can be satisfied with Eq. (4).

3.3. The state of water in membranes

The water is restrained on the polar surface, acrylamide group and strongly oriented. The acrylamide group consists of polar molecules with a strong tendency to form hydrogen bonds and has a high affinity for water. In this study, the states of water in

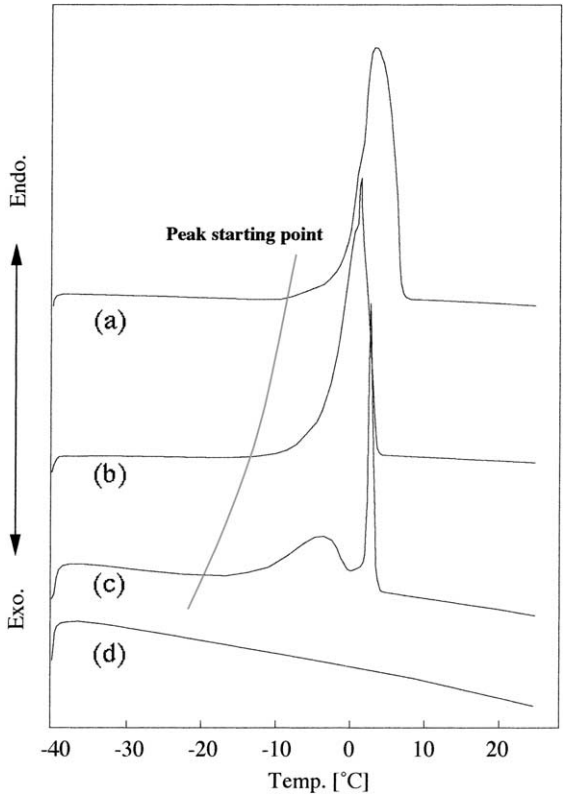

Fig. 3. DSC heating curves of water-swollen MMA series copolymer membranes: (a) 40/60-MMA/DMAA; (b) 50/50-MMA/DMAA; (c) 60/40-MMA/DMAA; (d) 70/30-MMA/DMAA. Heating rate = 5 K/min.

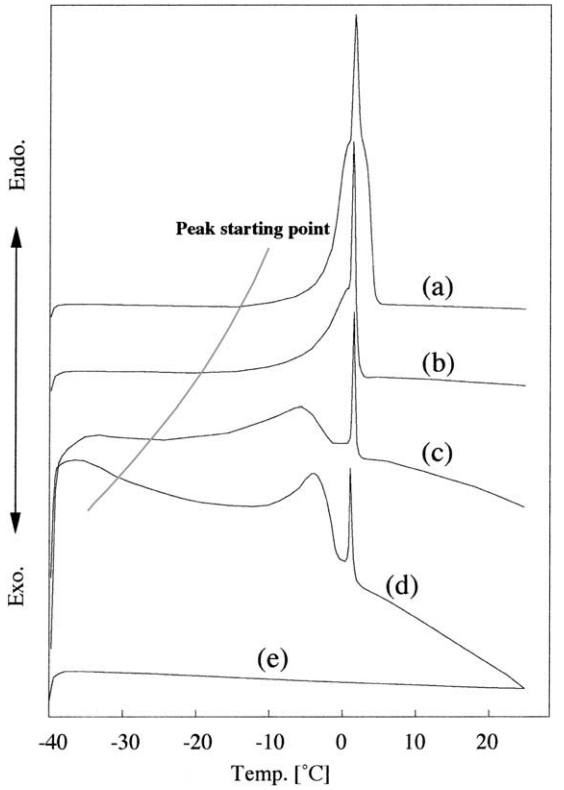

Fig. 4. DSC heating curves of water-swollen TMS series copolymer membranes: (a) 30/70-TMS/DMAA; (b) 40/60-TMS/DMAA; (c) 50/50-TMS/DMAA; (d) 60/40-TMS/DMAA; (e) 70/30 TMS/DMAA. Heating rate = 5 K/min.

the membranes were determined by DSC measurement. The DSC heating curves of the water-swollen poly(MMA-co-DMAA) and poly(TMS-co-DMAA) membranes are shown in Figs. 3 and 4, respectively. The heating rate of these DSC measurements was 5 K/min. For both copolymers, with the decrease in the water content of membranes, we found that the peak around 0 °C due to the melting of the freezing water is separated into two peaks; one remains close to 0 °C and the other shifts toward a lower temperature, about −7 °C. This result indicates that there is presumably weak interaction of the water with the polar surface. The interaction was remarkable in the poly(TMS-co-DMAA). For the 70/30-MMA/DMAA and 70/30-TMS/DMAA, no endothermic peak was observed in this DSC heating curve. This is due to a direct association with hydrophobic group of copolymer.

Fig. 5 shows the relationship between top-peak temperatures and starting temperatures in the melting of water sorbed in the studied copolymers as a function of water content. Top-peak temperatures nearly agreed in spite of changing of the water content. In the poly(TMS-co-DMAA) including the bulky hydrophobic pendant, however, the starting temperatures in the melting peak of water was detected from a lower temperature and water content. We consider that the existence of the bulky hydrophobic pendant depressed penetration of excess water into the membrane and that the water was more strongly oriented by the contribution of the bulky pendant. The amount of freezing water (W_{freezing}) in the heating process was calculated using the following equation:

$$W_{\text{freezing}} = \frac{Q^{\text{h}}}{\Delta H} \tag{5}$$

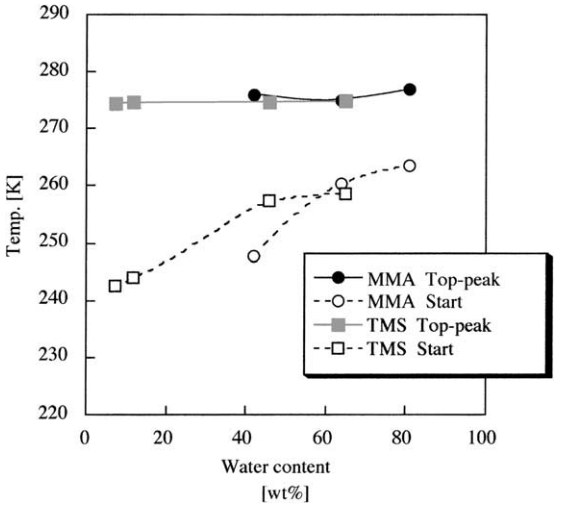

Fig. 5. Top-peak and starting temperature of melting of water sorbed in the copolymers as a function of water content. Heating rate = 5 K/min.

where Q^{h} is the heat capacity absorbed in the heating process, which is calculated from the peak area on the DSC chart. ΔH can estimate by using the difference of heat capacities of ice and super cooling water, ΔC_p.

$$\Delta H(T) = \Delta H(T = 273) - \int_{T}^{273} \Delta C_p \, \mathrm{d}t \qquad (6)$$

where $\Delta C_p = C_p$ (super cooling water) $- C_p$ (ice). We assumed that the water in the membrane and the bulk water is the same in relationship between transition temperature and the melting enthalpy. W_{non} was estimated by subtracting the weight of the freezing water ($W_{freezing}$) from the weight of water in the water-swollen membrane (W_{water}).

$$W_{non} = W_{water} - W_{freezing} \qquad (7)$$

Fig. 6 shows the relationship between the invaded water and the DMAA mole fraction in the copolymer membranes. In all the copolymer membranes, the non-freezing water (W_{non}) increased with the increase in the DMAA content. Especially, the non-freezing water of poly(MMA-co-DMAA) series increased almost linearly with the increase in the DMAA content. When the DMAA content was greater than 30 mol%, the freezing water ($W_{freezing}$) of the poly(MMA-co-DMAA) series remarkably increased. In addition, the remarkable increase in the

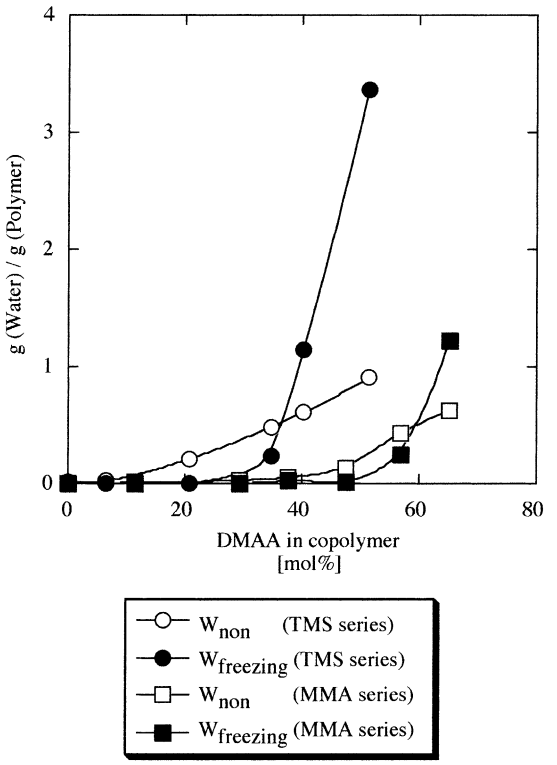

Fig. 6. Relationship between the entering water and DMAA mole fraction in the copolymer membranes.

poly(TMS-co-DMAA) series was observed for the DMAA content of more than 50 mol%. We considered that these results also depend on the contribution of the hydrophobic pendant.

3.4. Dissolved-oxygen permeation properties

Fig. 7 shows the comparison between the gaseous-oxygen permeability coefficients in dried membrane and in the dissolved-oxygen permeability coefficients in hydrated membrane. Results in the Fig. 7a and b correspond to values for the poly(MMA-co-DMAA) and poly(TMS-co-DMAA), respectively. The dissolved-oxygen permeability of the poly(MMA-co-DMAA) series increased with the increase of the DMAA content in the copolymer. The incorporation of water into the poly(MMA-co-DMAA) depends on the role of the hydrophobic pendant, that is, the excess water can not significantly enter the membrane up to about

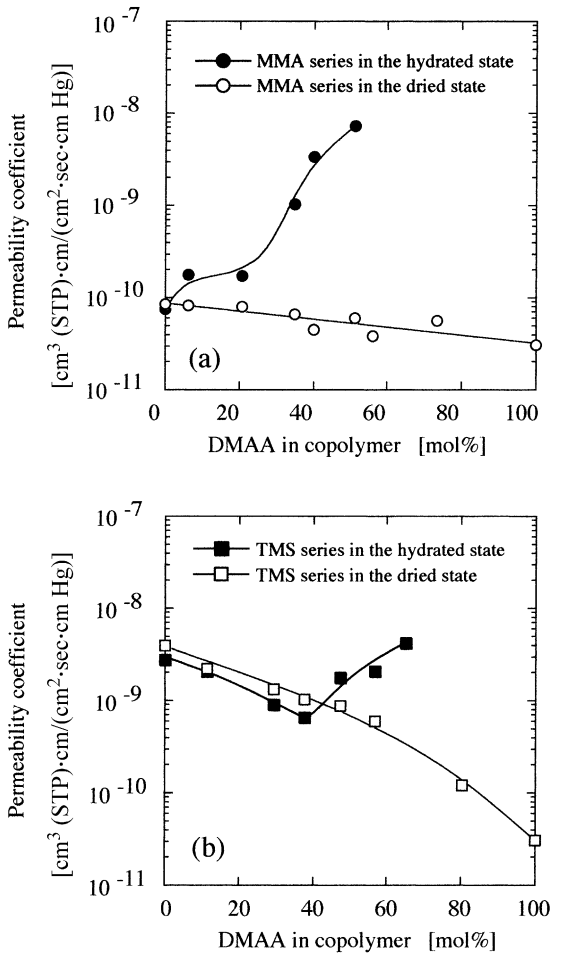

Fig. 7. Comparison between the gaseous-oxygen permeability coefficients in the dried membrane and the dissolved-oxygen permeability coefficients in the hydrated membrane: (a) poly(MMA-co-DMAA); (b) poly(TMS-co-DMAA).

20 mol% of the DMAA content due to the existence of the hydrophobic pendant of MMA. This result is closely related to the behavior of the freezing water ($W_{freezing}$) shown in Fig. 6. The dissolved-oxygen permeability of the poly(TMS-co-DMAA) showed nearly same the tendency with the oxygen permeability in the dried state up to about 40 mol% of the DMAA content. The dissolved-oxygen permeability of the poly(TMS-co-DMAA) decreased with the increase in the DMAA content up to about 40 mol%. We consider that this result depends on the result of the gaseous-oxygen permeability in the dried state because the water can scarcely enter into the membrane due to the effect of the bulky hydrophobic pendant (trimethylsilyl group). The dissolved-oxygen permeability coefficients of the poly(TMS-co-DMAA) up to 40 mol% of the DMAA content, however, were slightly low compared with the results of the gaseous-oxygen permeability coefficients in the dried state. We consider that some water, which entered the membrane, prevents the permeation of oxygen through the membrane and exists as oriented non-freezing water (W_{non}). Moreover, a sharp increase in the poly(TMS-co-DMAA) series was confirmed at the DMAA contents of more than 50 mol%. The point of this increase was the same as the inflection point of the freezing water ($W_{freezing}$). We believe that the dissolved-oxygen permeability depends on the amount of freezing water present in the membrane. In the water-swollen membranes, more than a 40 mol% DMAA content in the poly(MMA-co-DMAA) series membranes produced turbid membranes (50/50- and 40/60-MMA/DMAA; water content >60 wt.%). The 40/60-MMA/DMAA membrane was also brittle. In the poly(TMS-co-DMAA) series membranes, more than a 65 mol% DMAA content produced turbid and brittle membranes (30/70-TMS/DMAA; water content >60 wt.%). Moreover, the *d*-spacing of each hydrated membrane increased with the increase of water content. The increasing point of this *d*-spacing in the hydrated state was also the same as the inflection point of the dissolved-oxygen permeability and the freezing water ($W_{freezing}$). We believe that the existence of water spread polymer-chain space. In high water content membrane, we consider that the dissolved-oxygen permeate through the freezing water which exists in there. The dissolved-oxygen permeability behavior closely related to the state of water in the membranes and the physical property, such as the *d*-spacing.

3.5. Effects of heavy ion irradiation

Previously, the authors investigated the effect of heavy ion irradiation on the gas permeation of PET membrane, which is hydrophobic [24]. As a result, pores were formed in the PET membrane by heavy ion irradiation of a constant condition. Their gas permeation in the dried state increased and exhibited a Knudsen flow. We expected that the dissolved-oxygen permeability would increase by heavy ion irradiation

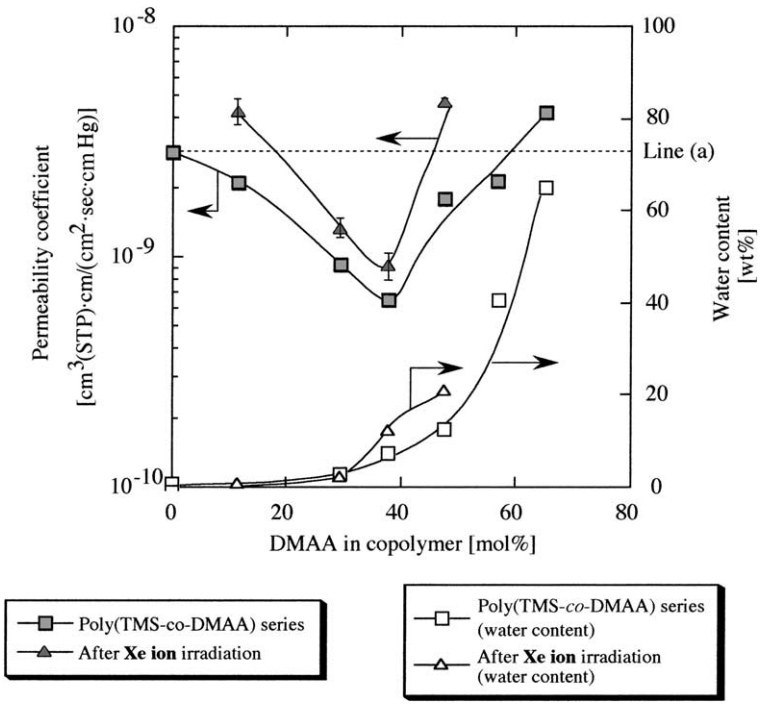

Fig. 8. Effects of ^{129}Xe ion irradiation on the water content and the dissolved-oxygen permeability coefficients of poly(TMS-co-DMAA) membranes at 35 °C. Line (a) represents the lowest desired oxygen permeability coefficient line for cornea.

and considered its application for CL and artificial dialysis membrane. The water content and the dissolved-oxygen permeability of the heavy ion-irradiated membrane are illustrated in Fig. 8. The irradiation beam was the Xe ion. The dotted line in the Fig. 8 shows the lowest desired oxygen permeability coefficient line for cornea. The dissolved-oxygen permeability of the Xe ion-irradiated copolymer membranes became higher compared with that of the untreated membranes. In the copolymer with low DMAA content, that is 90/10- and 70/30-TMS/DMAA, their water content did not increase by Xe ion irradiation. The PTMS homopolymer membrane became brittle by the Xe ion irradiation, therefore, various measurements were not done. The results of the GPC measurements of the Xe ion-irradiated membranes are shown in Table 3. The molecular weight (M_n and M_w) and the M_w/M_n ratio of the Xe ion-irradiated 90/10-TMS/DMAA became lower and greater than the untreated 90/10-TMS/DMAA, respectively. In low molecular weight polymers, generally, a large contribution to the segmental mobility comes from the chain ends, which are less constrained by chain connectivity requirements and are more mobile [30,31]. As the polymer's molecular weight decreases, the concentration of the chain ends increases. Therefore, the diffusivity of the penetrant increases with decreasing molecular weight. Based on these GPC measurement results, we confirmed that the cross-linking reaction occurred by the heavy ion irradiation. However, the fraction of the chain ends is expected to increase by damage caused by the Xe ion irradiation. We consider that the dissolved-oxygen permeability in the other Xe ion-irradiated copolymers

Table 3
Results of GPC measurement for Xe ion-irradiated membranes

Heavy ion-irradiated sample	$M_n \times 10^4$	$M_w \times 10^4$	M_w/M_n ratio
90/10-TMS/DMAA	7.0	410	58
70/30-TMS/DMAA	–[a]	–[a]	–[a]
60/40-TMS/DMAA	–[a]	–[a]	–[a]
50/50-TMS/DMAA	–[a]	–[a]	–[a]

[a] Insoluble in THF solvent.

of low water content, which is 70/30-TMS/DMAA, also increased with the increase of chain-ends produced by the Xe ion irradiation. In the copolymer with high DMAA content, that is 60/40- and 50/50-TMS/DMAA, the water content of the Xe ion-irradiated copolymer membranes also became higher compared with that of the untreated copolymer membranes. Fig. 9 shows the IR spectra of the untreated 50/50-TMS/DMAA membrane and Xe ion-irradiated 50/50-TMS/DMAA membrane. The peak at about 3400 cm^{-1}, that is the hydroxyl group peak, was significantly increased by the Xe ion irradiation. The IR spectra of the untreated 60/40-TMS/DMAA membrane and Xe ion-irradiated 60/40-TMS/DMAA membrane also showed same tendency. As reported in a previous paper, the *trans*-vinylene, carbonyl, hydroxyl group or terminal double bond was formed in the hydrophobic polymer by heavy ion irradiation [32]. We believed that the active radical generated by the heavy ion irradiation was oxidized in the atmosphere and hydroxyl groups were preferentially formed. In this study, no other chemical structural changes, except the hydroxyl group, were detected. We consider that the hydrophilic copolymer membranes with a high DMAA content preferentially took water vapor from the atmosphere and reached the increase of the dissolved-oxygen permeability.

Table 4
Comparison of the DMAA content determined by elemental analysis of a nitrogen atom in the untreated poly(TMS-co-DMAA) membranes with that in the Xe ion-irradiated poly(TMS-co-DMAA) membranes

Sample	DMAA content untreated (mol%)[a]	DMAA content heavy ion-irradiated (mol%)[a]
90/10-TMS/DMAA	11.5	10.6
70/30-TMS/DMAA	29.3	29.8
60/40-TMS/DMAA	37.8	39.3
50/50-TMS/DMAA	47.5	47.3
40/60-TMS/DMAA	56.8	56.6

[a] Determined the nitrogen content in the copolymer by elemental analysis using the combustion method.

Table 4 shows a comparison of the DMAA content (mol%) in the untreated copolymer membranes with that in the Xe ion-irradiated copolymer membranes. The mole fraction of DMAA in the copolymer, that is the DMAA content, was calculated from the nitrogen content that was determined by elemental analysis using the combustion method. Elemental analysis was carried out after all samples were immersed in water for a day. We were concerned about the elution of the monomer or oligomer because the polymer chain was broken by heavy ion irradiation. This value indicated, however, that elution of the monomer, formed by the

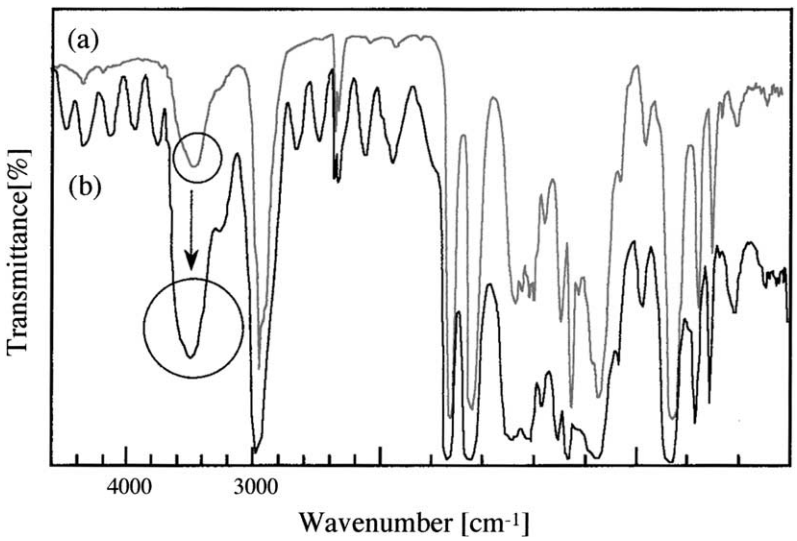

Fig. 9. IR spectra of the untreated 50/50-TMS/DMAA (a) and the Xe ion-irradiated 50/50-TMS/DMAA (b).

Xe ion irradiation, is hardly confirmed. In addition to there, the difference in the *d*-spacing of hydrated membrane between the untreated poly(TMS-co-DMAA) and the heavy ion-irradiated poly(TMS-co-DMAA) was found to be so minute that it was insignificant. The flexibility of membrane scarcely changes by heavy ion irradiation. We consider that the cross-linking structure formed by the heavy ion irradiation depressed spread of polymer-chain space and maintained flexibility. As these results, the dissolved-oxygen permeability coefficient of Xe ion-irradiated 90/10- and 50/50-TMS/DMAA membrane exceeded the lowest desired oxygen permeability coefficient line for cornea. Considering in view of above results and discussion, we consider that heavy ion irradiation can be applied as a useful tool in membrane modification.

4. Conclusions

The copolymer membranes in this study were synthesized by radical bulk copolymerization. Their morphology was analyzed using the monomer reactivity ratio and a transport model of copolymer membranes. As a result, the poly(MMA-co-DMAA) and poly(TMS-co-DMAA) membranes formed a random structure. In poly(TMS-co-DMAA), the structure is particularly comparable to the regular copolymer due to $r_1 r_2 \leq 1$.

The permeation behavior of the PMMA and PTMS homopolymers for dissolved-oxygen permeability was mainly carried out through the polymer chain. For poly(MMA-co-DMAA), the dissolved-oxygen permeability increased with increasing the DMAA content. For poly(TMS-co-DMAA), however, the dissolved-oxygen permeated mainly through the polymer chain up to 40 mol% of DMAA content due to effect of the bulky hydrophobic pendant (trimethylsilyl group). Then, the dissolved-oxygen permeability in the poly(TMS-co-DMAA) remarkably increased at DMAA contents of more than 50 mol% We believed that the dissolved-oxygen permeability coefficients in the hydrated state were slightly lower than the gaseous-oxygen permeability coefficients in the dried state because the existence of non-freezing water prevents the permeation of penetrant oxygen. Contribution of the hydrophobic pendant in the copolymer synthesized in hydrophobic and hydrophilic monomers plays an important role in the relationship between the absorbed water and permeability of penetrant. Moreover, the *d*-spacing of each hydrated membrane increased with the increase of the water content. The increasing point of *d*-spacing in the hydrated state was also the same as the inflection point of the dissolved-oxygen permeability and the freezing water (W_{freezing}). The dissolved-oxygen permeability behavior closely related to the state of water in membranes and physical property, such as *d*-spacing.

We attempted to irradiate the poly(TMS-co-DMAA) membranes with a heavy ion beam. For the ion beam irradiation, ^{129}Xe ions were supplied from a cyclotron. The dissolved-oxygen permeability of the Xe ion-irradiated copolymer membranes became higher compared with that of the untreated membranes. In the copolymer with high DMAA content, that is 60/40- and 50/50-TMS/DMAA, the water content of the Xe ion-irradiated copolymer membranes also became higher compared with that of the untreated copolymer membranes. In the result of FT-IR measurement, the peak at about 3400 cm^{-1}, that is the hydroxyl group peak, was significantly increased by Xe ion irradiation. We believe that the active radical generated by the heavy ion irradiation was oxidized in the atmosphere and hydroxyl groups were preferentially formed. In this study, increasing the dissolved-oxygen permeability in the hydrophilic membrane was accomplished by heavy ion irradiation. In addition, the *d*-spacing and flexibility of membrane scarcely changes by heavy ion irradiation. We consider that the cross-linking structure formed by the heavy ion irradiation depressed spread of polymer-chain space, and maintained flexibility. As these results, the dissolved-oxygen permeability coefficient of Xe ion-irradiated 90/10- and 50/50-TMS/DMAA membrane exceeded the lowest desired oxygen permeability coefficient line for supplying the oxygen cornea. In the near future, we expect that many applications and investigations utilizing heavy ion irradiation may emerge.

Acknowledgements

We would like to thank Dr. Masaru Hoshi and Mr. Mamoru Kobayashi, LINTEC Corporation, for their assistance in the GPC experiments.

The authors wish to dedicate this paper to their esteemed senior, Professor Dr. Patric Meares of the University of Exceter, on the occasion of his retirement. With all good wishes for the future.

References

[1] M.F. Refojo, F.L. Leong, Water-dissolved-oxygen permeability coefficients of hydrogel contact lenses and boundary layer effects, J. Membr. Sci. 4 (1979) 415.

[2] T. Kojima, S. Okazaki, Wettability of contact lenses, J. Jpn. Contact Lenses Soc. 40 (1998) 116.

[3] Y.C. Lai, A.C. Wilson, S.G. Zantos, Kirk Encyclopedia of Chemical Technology, 4th Edition, Vol. 7, Wiley, New York, 1993.

[4] R.M. Hodge, G.P. Simon, M.R. Whittaker, D.J.T. Hill, A.K. Whittaker, Free volume and water uptake in a copolymer hydrogel series, J. Polym. Sci. B Polym. Phys. 36 (1998) 463.

[5] T. Nakagawa, Y. Sugisaki, Transport properties of synthetic membranes having hydrophilic and hydrophobic structures, Membrane 16 (1991) 204.

[6] G. Friends, J. Kunzler, J. Mcgee, R. Ozark, Hydrogels based on copolymers of *N*-(2-hydroxyethyl)methacrylamide, 2-hydroxyethyl methacrylate and 4-*t*-butyl-2-hydroxycyclohexyl methacrylate, J. Appl. Polym. Sci. 49 (1993) 1869.

[7] Y.C. Lai, P.L. Valint Jr., Control of properties in silicone hydrogels by using a pair of hydrophilic monomers, J. Appl. Polym. Sci. 61 (1996) 2051.

[8] J. Crank, G.S. Park, Diffusion in Polymers, Academic Press, London, 1968.

[9] Y.C. Lai, Role of bulky polysiloxanylalkyl methacrylates in oxygen-permeable hydrogel materials, J. Appl. Polym. Sci. 56 (1995) 317.

[10] Y.C. Lai, The role of bulky polysiloxanylalkyl methacrylates in polyurethane–polysiloxane hydrogels, J. Appl. Polym. Sci. 60 (1996) 1193.

[11] J. Kunzler, R. Ozark, Hydrogels based on hydrophilic side-chain siloxanes, J. Appl. Polym. Sci. 55 (1995) 611.

[12] J. Brandrup, E. H. Immergut, Polymer Handbook, 3rd Edition, Wiley/Interscience, New York, 1989.

[13] H. Yoshida, T. Hatakeyama, H. Hatakeyama, Effect of water on the main chain motion of polysaccharide hydrogels, in: Viscoelasticity of Biomaterials, in: American Chemical Society Symposium Series, Vol. 489, Washington, 1991.

[14] T. Hatakeyama, H. Hatakeyama, K. Nakamura, Non-freezing water content of mono- and divalent cation salt of polyelectrolyte–water systems studied by DSC, Thermochim. Acta 253 (1995) 137.

[15] T. Hatakeyama, H. Yoshida, H. Hatakeyama, A differential scanning calorimetry study of the phase transition of the water–sodium cellulose sulfate system, Polymer 28 (1987) 1282.

[16] T. Hatakeyama, H. Yoshida, H. Hatakeyama, The liquid crystalline state of water–sodium cellulose sulfate systems studied by DSC and WAXS, Thermochim. Acta 266 (1995) 343.

[17] Y. Hirata, Y. Miura, T. Nakagawa, Oxygen permeability and the state of water in Nafion membranes with alkali metal and amino sugar counter-ions, J. Membr. Sci. 163 (1999) 357.

[18] K.F. Mueller, Thermotropic aqueous gels and solutions of *N*,*N*-dimethyl acrylamide–acrylate copolymers, Polymer 33 (1992) 3470.

[19] W.F. Lee, P.L. Yeh, Thermoreversible hydrogels. II. Effect of some factors on the swelling behavior of *N*,*N*-dimethyl acrylamide and *n*-butoxymethyl acrylamide copolymeric gels, J. Appl. Polym. Sci. 65 (1997) 909.

[20] M. Tamada, M. Yoshida, M. Asano, H. Omichi, R. Katakai, R. Spohr, J. Vetter, Thermoresponse of ion track pores in copolymer films of methacryloyl-L-alanine methyl ester and diethyleneglycol-bis-allylcarbonate, Polymer 33 (1992) 3169.

[21] M. Tamada, M. Yoshida, M. Asano, H. Omichi, R. Katakai, C. Trautmann, J. Vetter, R. Spohr, Sensitization of track etching in CR-39 by copolymerization with methacryloyl-L-alanine methyl ester, Nucl. Tracks Radiat. Measure. 20 (1992) 543.

[22] M. Yoshida, N. Nagaoka, M. Asano, H. Omichi, H. Kubota, K. Ogura, J. Vetter, R. Spohr, R. Katakai, Reversible on–off switch function of ion-track pores for thermoresponsive films based on copolymers consisting of diethyleneglycol-bis-allylcarbonate and acryloyl-L-proline methyl ester, Nucl. Instrum. Methods B 122 (1997) 39.

[23] M. Yoshida, M. Asano, A. Safranj, H. Omichi, R. Spohr, J. Vetter, R. Katakai, Novel thin film with cylindrical nanopores that open and close depending on temperature: first successful synthesis, Macromolecules 29 (1996) 8987.

[24] S. Takahashi, M. Yoshida, M. Asano, T. Tanaka, T. Nakagawa, Effect of heavy ion irradiation on gas permeability of poly(ethylene terephthalate) (PET) membrane, J. Appl. Polym. Sci., in press.

[25] C. Rogers, J.A. Meyer, V. Stannett, M. Szwarc, Studies in the gas and vapor permeability of plastic films and coated papers, Tappi 39 (1956) 737.

[26] N. Minoura, Y. Fujiwara, T. Nakagawa, Permeability of synthetic poly(amino acid) membranes to oxygen dissolved in water, J. Appl. Polym. Sci. 24 (1979) 965.

[27] T. Nakagawa, Oxygen permeability of membrane materials for contact lenses, J. Jpn. Contact Lenses Soc. 30 (1988) 1.

[28] K. Nagai, A. Higuchi, T. Nakagawa, Gas permeability and stability of poly(1-trimethylsilyl-1-propyne-co-1-phenyl-1-propyne) membranes, J. Polym. Sci. B Polym. Phys. 33 (1995) 289.

[29] J.A. Barrie, K. Munday, Gas transport in heterogeneous polymer blends. II. Blends of polydimethylsiloxane and poly(ethylene-co-propylene) elastomers, J. Membr. Sci. 13 (1983) 197.

[30] K. Toi, D.R. Paul, Effect of polystyrene molecular weight on the carbon dioxide sorption isotherm, Macromolecules 15 (1982) 1104.

[31] K. Ghosal, B.D. Freeman, Gas separation using polymer membranes: an overview, Polym. Adv. Technol. 5 (1994) 673.

[32] Y. Hama, K. Hamanaka, H. Matsumoto, T. Takano, H. Kudou, M. Sugimoto, T. Suguchi, The distribution profile of the chemical structural changes in ion-irradiated polyolefins, Radiat. Phys. Chem. 48 (1996) 549.